

SAND98-1066 C  
SAND-98-1066C

MAGNETIC MODULATIONS OF OPTICAL AND TRANSPORT  
PROPERTIES OF N-DOPED COUPLED DOUBLE QUANTUM WELLS

S. K. LYO<sup>†</sup>, D. HUANG<sup>§</sup>, J. A. SIMMONS<sup>†</sup>, AND N. E. HARFF<sup>#</sup>

SANDIA NATIONAL LABORATORIES<sup>†</sup>, AIR FORCE RESEARCH LABORATORY<sup>§</sup>,  
ALBUQUERQUE, NM, USA, MAX PLANCK INSTITUTE<sup>#</sup>, STUTTGART, GERMANY

E-mail: sklyo@sandia.gov

CONF-980829--

Magnetoquantum resistance (MR) in a perpendicular magnetic field ( $B_{\perp}$ ) and photoluminescence (PL) spectra are shown to be sensitively modulated by an in-plane field ( $B_{\parallel}$ ) due to the  $B_{\parallel}$ -induced anticrossing of the energy-dispersion curves of the two quantum wells (QWs). Using a self-consistent density functional theory, we find very different  $B_{\parallel}$ -evolutions of the PL spectra for symmetric and asymmetric double QWs consistent with recent data. The MR is calculated using a linear response theory. The results consist of a superposition of two series of MR oscillations represented by ridges running nearly perpendicular to each other in the  $B = (B_{\parallel}, B_{\perp})$  plane. Our data from GaAs/AlGaAs double QWs agree with this behavior.

## 1 Introduction

Double quantum wells (DQWs) display many interesting properties due to tunneling, absent in single QWs. In a purely in-plane magnetic field  $B_{\parallel}$  in the x direction, the wave vector  $k = (k_x, k_y)$  is a good quantum number except that  $k_y$  is displaced in the two QWs by  $\Delta k_y \approx d/\ell_{\parallel}^2$  where  $d$  is the center-to-center distance between the QWs and  $\ell_{\parallel} = (\hbar c/eB_{\parallel})^{1/2}$ . This can be seen from the Hamiltonian

$$H = -\frac{\hbar^2}{2m_{\parallel}^*} \frac{\partial^2}{\partial x^2} + \frac{\hbar^2}{2m_{\parallel}^*} [k_y + \frac{e}{\hbar c} A_y]^2 - \frac{\hbar^2}{2m_z^*} \frac{\partial^2}{\partial z^2} + V(z), \quad (1)$$

where  $A_y = B_{\parallel}z$  is the vector potential and  $V(z)$  is the confinement potential [1]. The energy dispersion parabolas of the two QWs anticross and split into two branches as shown in Fig.1 for symmetric DQWs. The gap  $\Delta_{\text{SAS}}$  passes through the chemical potential  $\mu$  (thick horizontal line) with increasing  $B_{\parallel}$  and is negligibly small for the holes due to the large heavy hole mass  $m_z^*$ . However, the in-plane hole mass is not large, yielding considerable curvatures for the dispersion. The samples considered here are GaAs/Al<sub>0.3</sub>Ga<sub>0.7</sub>As DQWs.

MASTER

DISTRIBUTION OF THIS DOCUMENT IS UNLIMITED

## **DISCLAIMER**

This report was prepared as an account of work sponsored by an agency of the United States Government. Neither the United States Government nor any agency thereof, nor any of their employees, makes any warranty, express or implied, or assumes any legal liability or responsibility for the accuracy, completeness, or usefulness of any information, apparatus, product, or process disclosed, or represents that its use would not infringe privately owned rights. Reference herein to any specific commercial product, process, or service by trade name, trademark, manufacturer, or otherwise does not necessarily constitute or imply its endorsement, recommendation, or favoring by the United States Government or any agency thereof. The views and opinions of authors expressed herein do not necessarily state or reflect those of the United States Government or any agency thereof.

## **DISCLAIMER**

**Portions of this document may be illegible electronic image products. Images are produced from the best available original document.**

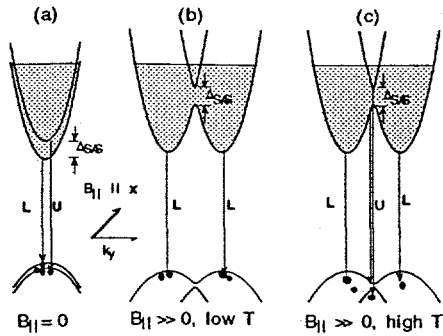


Figure 1. Anticrossing in symmetric DQWs and the transitions from the upper (U) and lower (L) branches.

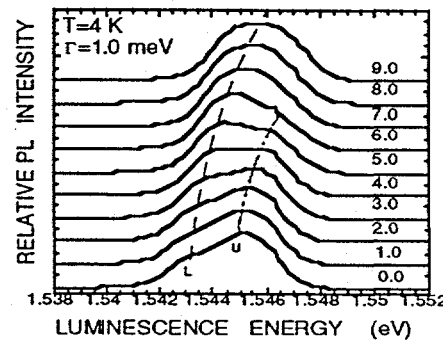


Figure 2.  $B_{\parallel}$ -evolution of the PL spectra from sample 1 for  $B_{\parallel}$  from 0 to 9 T.

## 2 $B_{\parallel}$ -Evolution of the PL Spectra

Eq. (1) is solved using a self-consistent density functional theory including the Hartree and exchange-correlation potentials [2]. The PL spectra are calculated using the formalism of Ref. 3 and assuming that the damping  $\Gamma$  is constant independent of the energy and is the same for the electrons and holes. The PL spectra are determined by the square of the wave function overlap times the joint spectral density of the electrons and the photogenerated holes averaged over their occupation probabilities given by the Fermi-Dirac and Boltzmann distributions.

The theory is applied to symmetric DQWs (sample 1) with 100 Å wells, a 35 Å center barrier, and 100% ionized delta dopants inside the outer barriers at a distance 50 Å from the outer interfaces with a density  $1.2 \times 10^{11}/\text{cm}^2$  each. Calculated PL spectra are displayed in Fig. 2 for  $0 \leq B_{\parallel} \leq 9$  T [4]. The spectra have two peaks at low  $B_{\parallel}$ 's. The upper peak (U) disappears at 5 T. The U-peak appears to be stronger because it rests at the tail of the lower peak (L). The double to single peak behavior can be understood from Fig. 1: at  $B_{\parallel} = 0$ , two strong PL peaks U and L arise from  $k_y = 0$  area near the bottoms of the upper and lower branches. At  $B_{\parallel} = 5$  T, however, U disappears because the holes are depopulated from the  $k_y = 0$  area. At a higher temperature, U disappears at a higher  $B_{\parallel}$  as seen from Fig. 1(c).

Figures 3 and 4 display the anticrossing and the PL spectra for asymmetric DQWs (sample 2) with the same structure as sample 1 but with a total electron density  $6.0 \times 10^{11}/\text{cm}^2$  and a 6 kV/cm electric field. In this case, the holes are in the right QW. The U peak is strong at  $B_{\parallel} = 0$  and arises from the intrawell transitions inside the right QW as illustrated in Fig. 3(a). The L peak arises from the interwell transitions and is weak. At high  $B_{\parallel}$ 's, the U peak becomes weak because the holes are not available and is replaced by a strong L peak as seen from Figs. 3(c) and 4. The behavior in Fig. 2 and 4 is consistent with recent observation [5].

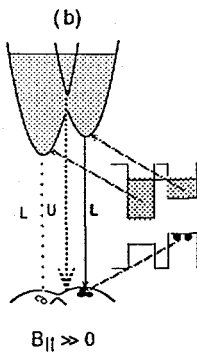
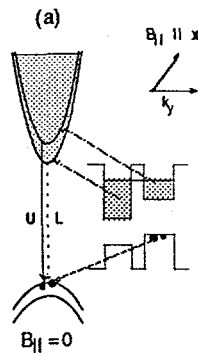


Figure 3. Anticrossing in asymmetric DQWs and the optical transitions from the upper (U) and lower (L) branches.

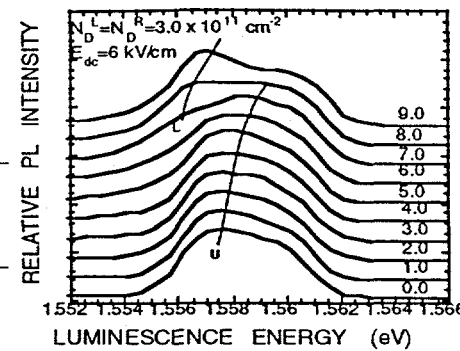


Figure 4.  $B_{\parallel}$ -evolution of the PL spectra from sample 2 for  $B_{\parallel}$  from 0 to 9 T.

## 2 Magnetoresistance ( $R_{xx}$ ) Oscillations in a Tilted Magnetic Field

In a tilted magnetic field, the vector potential is given by  $A_y = B_{\perp}x - B_{\parallel}z$ . We have calculated  $R_{xx}$  using a linear response theory. The Hamiltonian consists of 1) the Landau level (LL) energies  $(n+1/2)\hbar\omega_c$  of the two QWs due to  $B_{\perp}$  in the absence of tunneling plus 2) the tight-binding tunneling integral  $J_0 L(n_1, n_2)$ . Here  $J_0$  is the field-free tunneling integral which equals half the gap energy  $\Delta_{SAS}$  and  $L(n_1, n_2)$  is the overlap between the LL harmonic wave functions  $n_1$  and  $n_2$  belonging to QW1 and QW2. The role of  $B_{\parallel}$  is to displace the centroids  $= \ell_{\perp}^2 k_y$  of the two LLs by  $\Delta k_y \simeq d/\ell_{\parallel}^2$  relative to each other and induce nonzero coupling for  $L(n_1, n_2)$  for  $n_1 \neq n_2$  [6].

Here  $\ell_{\perp} = (\hbar c/eB_{\perp})^{1/2}$ . The conductivity is given by [7]

$$\sigma_{\alpha,\alpha} = \frac{e^2 \hbar}{\ell_{\perp}^2 L_z} \sum_{\gamma,\gamma'} | \langle \gamma | v_{\alpha} | \gamma' \rangle |^2 \int_{-\infty}^{\infty} [-f(z)'] \rho_{\gamma}(z) \rho_{\gamma'}(z) dz, \quad (2)$$

where  $f(z)$  is the derivative of the Fermi function,  $\gamma$  is the eigenstate,  $v$  the velocity operator, and  $L_z$  is the sample size in the  $z$ -direction. For the spectral density  $\rho_{\gamma}(z)$ , we use a Gaussian function centered at each eigenvalue with a constant root mean square deviation  $\Gamma$ , where  $\Gamma = 0.5 \eta \hbar \omega_c / B_{\perp}^{1/2}$ . Here  $\eta$  is a parameter which depends on the system [7].

In Figs. 5 and 6, we display the calculated  $R_{xx}$  for  $\eta = 0.2$  and the data from sample 3 with 150 Å wells, 15 Å center barrier,  $J_0 = 1.15$  meV, and the electron densities  $1.9 \times 10^{11}/\text{cm}^2$ , and  $1.0 \times 10^{11}/\text{cm}^2$ . The quantity  $\eta$  determines the size and the sharpness of the resistance peaks in Fig. 5.

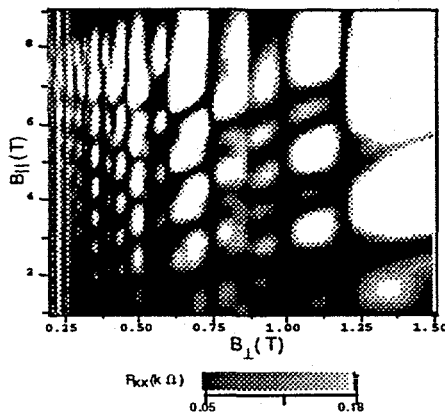


Figure 5. Calculated  $R_{xx}$  for sample 3.

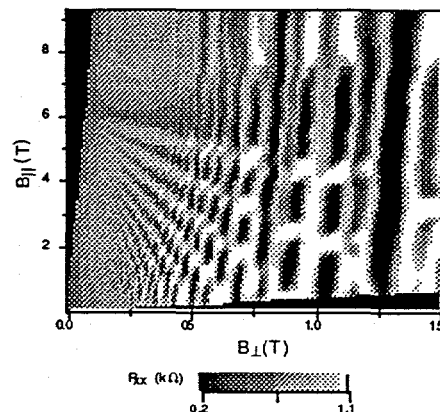


Figure 6.  $R_{xx}$  data from sample 3 [8].

$R_{xx}$  is much lighter in Fig. 5 than in Fig. 6 and is of the same order of magnitude.  $R_{xx}$  can be understood in the following way. The cyclotron mass in the upper (lower) branch decreases (increases) with increasing  $B_{\parallel}$  at  $B_{\perp} = 0$  [7]. Thus, the LLs in the upper (lower) branch sweep up (down) across  $\mu$  with increasing  $B_{\parallel}$  at a fixed  $B_{\perp}$ . The ridges running downward (upward) diagonally from left to right are due to the Fermi level crossing of the LLs in the upper (lower) branch. The  $R_{xx}$  maxima are produced when the two sets of the ridges intersect [7, 8].  $\mu$  is inside the gap for  $6.4 < B_{\parallel} < 7$  T. The ridges from the lower branch converge to the point  $B_{\parallel} \approx 6.4$  T at  $B_{\perp} = 0$  where  $\mu$  touches the bottom of the upper branch.

#### Acknowledgments

This work was supported by U.S. DOE under Contract No. DE-AC04-94AL85000.

#### References

1. S. K. Lyo, *Phys. Rev. B* **50**, 4965 (1994).
2. L. Hedin and B. I. Lundqvist, *J. Phys. C: Solid St. Phys.* **4**, 2064 (1971).
3. S. K. Lyo and E. D. Jones, *Phys. Rev. B* **38**, 4113 (1988).
4. D. Huang and S. K. Lyo, unpublished.
5. Y. Kim et al., *The Physics of Semiconductors*, ICPS 23, Edited by M. Scheffler and R. Zimmermann, p.1859 (World Scientific, Singapore, 1996) and unpublished.
6. J. Hu and A. H. MacDonald, *Phys. Rev. B* **46**, 12554 (1992).
7. S. K. Lyo, N. E. Harff, and J. A. Simmons, *Phys. Rev. B* **58**, 1572 (1998).
8. N. E. Harff et al., *Phys. Rev. B* **55**, R13405 (1997).

Sandia is a multiprogram laboratory operated by Sandia Corporation, a Lockheed Martin Company, for the United States Department of Energy under contract DE-AC04-94AL85000.